Examination of H-bridge Resonant Converter using Passivity-Based Control

Y.Lu, K.W.E.Cheng, S.L.Ho, J.F.Pan
Power Electronics Research Centre
Department of Electrical Engineering
The Hong Kong Polytechnic University
Hung Hom, Hong Kong

Abstract

This paper examines the H-bridge converter usin g Passivity based control. The nonlinearity of resonant type H-bridge converter is poor and therefore the dynamic performance of the converter is weak. Using simple PI control, the transient response is not satisfactory. The passivity based control is first derived for the H-bridge converter. The parameter estimation is examined and the comparison with the POI control is illustrated.

Key words: phase shift resonant converter, passivity, adaptive control

I Introduction

H-bridge converter is widely used for handling large power in DC/DC converter series. Among full bridge converters with different control laws or circuit topologies, the phase shift H-bridge resonant converter (we refer it as PSHRC below) has the advantage of inherent short circuit protection characteristic and high conversion efficiency, the transformer employed in the converter would not be saturated [1],[2],[3],[4]. Fig. 1 shows the schematic diagram of the PSHRC. The two IGBT components in each leg of the H Bridge are switched alternatively with almost 50% duty ratio. The switching pulses to the two legs have a phase angle α. The output voltage of the full bridge can be regulated via changing the angle αas shown in Fig. 2.

The passivity approach is a method following the idea of energy. It includes two steps: energy shaping and damping injection. Energy shaping is to regulate the energy flow of the system as what is desired. The second step is to reform the dynamics of the system. Passivity-based control (PBC) makes the system more robust [7], [8], [9],[10].

Recently PBC was applied to DC-DC converters [5], UPS [11] and many other converters.

An adaptive algorithm is derived to estimate the output load resistance; this feature allows us to avoid using an extra output current sensor. Only output voltage feedback is required for the PBC algorithm, thus the control system is simplified. A 1。4 kW PSHRC with PBC controller was developed. The laboratory experiments were carried out based on a DSP system and the experimental results indicate the perfect dynamic performance and stability of the system.

The controller is firstly simulated with Simulink/Matlab and tested by using a 1.4 kW PSHRC based on a DSP system. Satisfactory results are obtained.

Ⅱ Formulation of equations

Fig. 1 shows the schematic diagram of the PSHRC discussed in this paper, the state space equations of the resonant tank and the output filter of the converter are built as follows:

$$L_r \frac{di_r}{dt} = -v_{cr} - kv_1 sign(i_r) + v_i \quad (1)$$

$$C_r \frac{dv_{cr}}{dt} = i_r \quad (2)$$

$$L \frac{di_1}{dt} = v_1 - v_0 \quad (3)$$

$$C_1 \frac{dv_1}{dt} = k \cdot abs(i_r) - i_1 \quad (4)$$

$$C_2 \frac{dv_0}{dt} = i_1 - \frac{v_0}{r} \quad (5)$$

Where i_r is the resonant current through inductor L_r,

v_{cr} is the voltage across the resonant capacitor c_r, k is the turn ratio of the transformer, $k=N_p/N_s$. V_1 and i_1 are the voltage across the capacitor c_1 and the current through the inductor L respectively. V_0 is the output voltage supplying the load. L_r is actually the sum of the resonant inductor and the leakage inductor of the transformer and C_r is the resonance capacitor. The resonant tank is characterized by its resonant frequency denoted by $f_0 = \frac{1}{2\pi\sqrt{LrCr}}$. C_1 is the capacitor used for absorbing the resonant current and avoiding the duty cycle loss caused by the conduction overlap of D_1~D_4 . Inductor L and capacitor C_2 construct a lower pass filter. The load is represented by a purely resistive element r. V_i is the control input signal, the frequency of it is constant and the electrical phase angle α is controllable as shown in Fig. 2. We control the output voltage v_0 by regulating α. E is the input DC voltage of the converter.

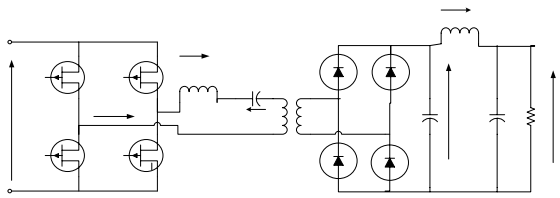

Fig 1 Schematic diagram of the PSHRC

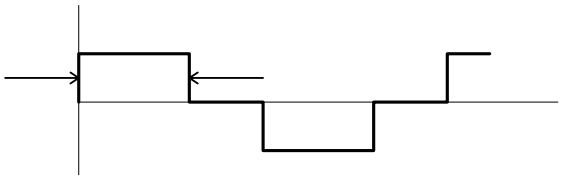

Fig 2 The voltage waveform of the PSHRC

The system described by Eqns (1-5) is a fifth order nonlinear system to convert v_i into v_o, where v_o is the only measurable signal and the output load represented here as a pure resistive element is constant but unknown. The control objective is to asymptotically regulate the output voltage v_o to some desired constant value $v_0>0$.

Ⅲ Development of the Modeling for PBC Converter

The model can be divided into two subsystems. We refer to Eqns (1)，（2） as the resonant tank and to Eqns (3)，(4), (5) as the output filter system. The models of the two subsystems will be discussed respectively.

A. Model analysis of the resonant tank

The waveform of the input signal v_i is shown as Fig. 2, where α is the phase angle, $0\le\alpha\le\pi$. The frequency of the signal is the switching frequency of the full bridge denoted as fs, the signal can be looked as the sum of each harmonic component by Fourier analysis. The amplitude of the first harmonic of the signal is $2/\pi(1-\cos\alpha)E$, where E is the DC link voltage, it can be seen that the voltage of the first harmonic increases with larger phase angle α. As the magnitude of the first harmonic component of the input signal is much greater than that of another order harmonic components and the fundamental frequency is very close to the resonant frequency characterized by $f_o=1/2\pi\sqrt{(L_rC_r)}$, under this circumstance the fundamental voltage across L_r and C_r almost cancel each other. The current generated by the first harmonic component of the input signal is much greater than that generated by other order harmonic components, therefore the modeling of the resonant tank circuit can be simplified by applying fundamental harmonic approximation of the system.

The experimental waveform shown in Fig. 4 verifies that the resonant current is quite sinusoidal with the fundamental frequency.

The model of the resonant tank circuit is given by

$$L_r\frac{di_r}{dt} = -v_{cr} - v_{pf} + v_{if} \tag{6}$$

$$C_r\frac{dv_{cr}}{dt} = i_r \tag{7}$$

where v_{if} and v_{pf} are the fundamental component of the input signal and primary voltage of the transformer respectively.

Now the, by ignoring the low order harmonics of the resonant current, that is quite true for resonant converter when the resonant frequency is very close to the

switching frequency, the resonant current is assumed to be:

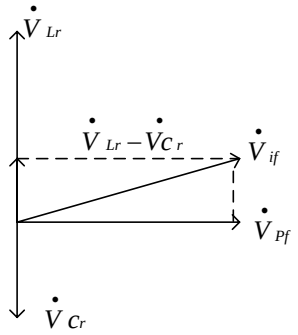

Fig. 3 Voltage phasor diagram of the resonant tank

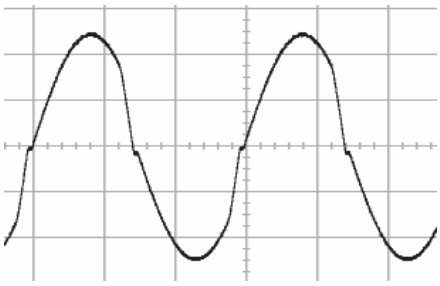

Fig. 4 Experimental Resonant current waveform

$$i_r = \mathrm{I_m}\sin\omega t \tag{8}$$

Then the voltage across L_r is:

$$v_{Lr} = \omega L_r I_m \sin(\omega t + 90°) = v_{Lrm}\sin(\omega t + 90°) \tag{9}$$

The voltage across C_r is:

$$v_{cr} = v_{rm}\sin(\omega t - 90°) \tag{10}$$

Where $v_{Lrm}=I_m\omega L_r$, $v_{rm}=I_m/\omega C_r$

The primary voltage of the transformer is:

$$v_p = kv_1 \mathrm{sign}(i_r) \tag{11}$$

Its fundamental component is:

$$v_{pf} = kv_1\frac{4}{\pi}\sin\omega t = v_{pm}\sin\omega t \tag{12}$$

where $v_{pm} = \dfrac{4kv_1}{\pi}$

Hence we can get a voltage phasor diagram as shown in Fig3 from Eqns (6), (7), (8), (9), (10), (11), (12). The voltage balance equation is written as:

$$\dot{V}_{if} = \dot{V}_{pf} + (\dot{V}_{Lr} - \dot{V}_{cr})$$

The peak values of these voltages satisfy:

$$\left[\frac{2}{\pi}(1-\cos\alpha)E\right]^2 = (\frac{4}{\pi}kv_1)^2 + I_m^2(\omega L_r - \frac{1}{\omega C_r})^2$$

$$\cos\alpha = 1 - \frac{\pi}{2E}\sqrt{\left(\frac{4}{\pi}kv_1\right)^2 + I_m^2\left(\omega L_r - \frac{1}{\omega C_r}\right)^2} \tag{13}$$

Where $0\le\alpha\le\pi$, $kv_1<E$. Eqn (13) reveals the relationship among phase angle,α,v_1, and I_m under steady states.

B. Model analysis of the output filter

As shown in Fig1, we take the rectified current and the output voltage v_0 as the input signal and output signal of the subsystem respectively; and then Eqns (3), (4), (5) can be written as:

$$D\dot{X} + RX + JX = U \tag{14}$$

Where I=kabs(i_r),

$$D = \begin{bmatrix} L & 0 & 0 \\ 0 & C_1 & 0 \\ 0 & 0 & C_2 \end{bmatrix} \quad X = [i_1, v_1, v_0]^T \quad U = [0, I, 0]^T$$

$$J = \begin{bmatrix} 0 & -1 & 1 \\ 1 & 0 & 0 \\ -1 & 0 & 0 \end{bmatrix}$$

It can be seen that R is positive definition matrix and matrix D and matrix J satisfy J^T=-J, $D^T = D$.

C. Cascade of the subsystems

The two subsystems of the PSHRC are quite different in their electric inertia, i.e. the time constant.

Because of high frequency switching, the time constant of the resonant tank circuit is very small. The resonant frequency of the converter discussed in this paper is fs=33 kHz. Generally the time constant of the output fitter is much long than that of it to obtain smooth output voltage. Hence we can make this consideration, which reduce the dynamics of the resonant tank circuit to a static non-linearity in cascade with an output

passive filter. Then the relationship of the phase angle αand the peak value of the resonant current I_m is given by

$$\mathrm{Im}=\frac{\left\{\left[(1-\cos\alpha)E\frac{2}{\pi}\right]^2-\left(\frac{4}{\pi}kv_1\right)^2\right\}^{\frac{1}{2}}}{\omega L_r-\frac{1}{\omega C_r}} \qquad (15)$$

The average value of the rectified secondary current of the transformer can be looked as the input signal of the output passive filter. From now on we assume

$$I=k\frac{2}{\pi}\mathrm{Im} \qquad (16)$$

IV Controller Design for PBC

A Controller design

As discussed, if we take the average value of the rectified secondary currant of the transformer as the control signal of the converter, an expression for αis given by (13) and (16) respectively. We consider the model described by (14):

$$D\dot{X}+JX+RX=U \qquad (17)$$

Let the output variables be

$$Y=X \qquad (18)$$

Now, define an energy storage function

$$V=\frac{1}{2}X^TDX=\frac{1}{2}Li_1^2+\frac{1}{2}C_1v_1^2+\frac{1}{2}C_2v_0^2$$

It's time derivative along (17) and (18) gives

$$\dot{V}=X^TD\dot{X}=-X^TRX+U^TY<U^TY$$

So the system is strictly passive, the external energy only supplies the energy dissipated in the load. In accordance with the passivity approach, the control law can be derived. We assume the error variables $\tilde{i}_1=i_1-i_{1d}$, $\tilde{v}_1=v_1-v_{1d}$, $\tilde{v}_0=v_0-v_{0d}$; where i_{1d}, v_{1d} and v_{od} are the desired values of i_1, v_1 and v_0 respectively. Substituting them into equation (17):

$$D\dot{\tilde{X}}=-(J+R)\tilde{X}+U-D\dot{X}_d-(J+R)X_d$$

$$=-(J+R)\tilde{X}+\psi \qquad (19)$$

Where

$$\tilde{X}=\begin{bmatrix}\tilde{i}_1 & \tilde{v}_1 & \tilde{v}_0\end{bmatrix}^T \qquad X_d=\begin{bmatrix}i_{1d} & v_{1d} & v_{0d}\end{bmatrix}^T$$

$$\psi=U-D\dot{X}_d-(J+R)X_d \qquad (20)$$

For this error model described by equation (19), the storage function is defined as:

$$P(x)=\frac{1}{2}\tilde{X}^TD\tilde{X}=\frac{1}{2}L\tilde{i}_1^2+\frac{1}{2}C_1\tilde{v}_1^2+\frac{1}{2}C_2\tilde{v}_0^2$$

Hence

if, $D\dot{\tilde{X}}=-(J+R)\tilde{X}+\psi$, $X=\begin{bmatrix}i_1, v_1, v_0\end{bmatrix}^T$

$$D^T=D, \qquad J^T=-J$$

then

$$\frac{dP}{dt}=\dot{P}=\tilde{X}^TD\dot{\tilde{X}}=-\tilde{X}^TR\tilde{X}+\psi^T\tilde{X}$$

Proving:

$$\dot{P}=\frac{1}{2}(\dot{\tilde{X}}^TD\tilde{X}+\tilde{X}^TD\dot{\tilde{X}})$$

($\tilde{X}^TD\tilde{X}$) is actually scalar, it should be equal to its transposed matrix,

$$\dot{\tilde{X}}^TD\tilde{X}=(\dot{\tilde{X}}^TD\tilde{X})^T=(D\tilde{X})^T\dot{\tilde{X}}$$

$$=\tilde{X}^TD^T\dot{\tilde{X}}=\tilde{X}^TD\dot{\tilde{X}}$$

Therefore

$$\dot{P}=\tilde{X}^TD\dot{\tilde{X}}=\tilde{X}^T[-(J+R)\tilde{X}+\psi]$$
$$=-\tilde{X}^TJ\tilde{X}-\tilde{X}^TR\tilde{X}+\tilde{X}^T\psi$$

($\tilde{X}^T\psi$) and ($\tilde{X}^TJ\tilde{X}$) are both scalar,

Thus $\tilde{X}^T\psi=(\tilde{X}^T\psi)^T=\psi^T\tilde{X}$

$$\tilde{X}^TJ\tilde{X}=(\tilde{X}^TJ\tilde{X})^T=(J\tilde{X})^T\tilde{X}$$

$$=\tilde{X}^TJ^T\tilde{X}=-\tilde{X}^TJ\tilde{X}$$

Hence $\tilde{X}^TJ\tilde{X}=0$

$$\dot{P} = -\tilde{X}^T R\tilde{X} + \psi^T \tilde{X}$$

It's time derivative along (19) gives

$$\dot{P} = \tilde{X}^T D\dot{\tilde{X}} = -\tilde{X}^T R\tilde{X} + \psi^T \tilde{X} \qquad (21)$$

The detail proving of (21) is given out in appendix. R, as we know, is positive definite, then let Ψ be the generalized control of the error system to ensure the error system of the PSHRC to be strictly passive. Here $P(x)$ taking place of the original storage function is called energy shaping. $P(x)$ can also be looked as the Lyaponov fundion of the error model. As a consequence, if we design the control law properly to make sure $\dot{P} < 0$, the system is stable asymptotically.

That is $\lim_{t\to\infty} \tilde{X} = 0,$ namely $v_0 \to v_{od}$

Now we perform the damping injection. Let

$$\psi = -C\tilde{X} \qquad (22)$$

where $C = \begin{bmatrix} 0 & 0 & 0 \\ 0 & 0 & 0 \\ 0 & 0 & c \end{bmatrix} \qquad c > 0$

C is a positive definition matrix. Substituting (22) into (21), we get $\dot{P} = -\tilde{X}^T (R + C)\tilde{X} < 0$

Hence the control law given by (20) and (22) can be specified as following equation group:

$$\begin{cases} L\dfrac{di_{1d}}{dt} + v_{0d} - v_{1d} = 0 \\ C_1\dfrac{dv_{1d}}{dt} + i_{1d} - I = 0 \\ C_2\dfrac{dv_{0d}}{dt} - i_{1d} + \dfrac{1}{r}v_{0d} - c(v_0 - v_{0d}) = 0 \end{cases}$$

The reference of the output voltage is $v^*=v_{0d}=$const, substituting it into the equation group, the control law is obtained after some algebraic and derivative manipulations:

$$I = \frac{1}{r}v^* + c(v^* - v_0) - cLC_1\frac{d^2 v_0}{dt^2} \qquad (23)$$

The structure of the controller is simple though the design theory is complicated.

B. Load estimation and adaptation

We will present the adaptive version of the controller using the PBC approach. Suppose the value of the resistance load is constant but unknown, it can be estimate by adaptation approach. Let

$$\frac{1}{r} = \theta, \qquad \theta = \hat{\theta} - \tilde{\theta}$$

Where $\hat{\theta}$ is the estimation value of θ

$\tilde{\theta}$ is the estimation error.

We assume

$$R_1 = \begin{bmatrix} 0 & 0 & 0 \\ 0 & 0 & 0 \\ 0 & 0 & \hat{\theta} \end{bmatrix}, \qquad R_2 = \begin{bmatrix} 0 & 0 & 0 \\ 0 & 0 & 0 \\ 0 & 0 & \tilde{\theta} \end{bmatrix},$$

Then

$$R = R_1 - R_2 \qquad (24)$$

Substitute (24) into the last term of the right side of (19)

$$D\dot{\tilde{X}} + (J + R)\tilde{X} = U - D\dot{X}_d - JX_d - R_1X_d + R_2X_d$$

Let

$$D\dot{\tilde{X}} + (J + R)\tilde{X} - R_2X_d = -C\tilde{X} \qquad (25)$$

Then

$$U - D\dot{X}_d - JX_d - R_1X_d = -C\tilde{X} \qquad (26)$$

Where $C = \begin{bmatrix} 0 & 0 & 0 \\ 0 & 0 & 0 \\ 0 & 0 & c \end{bmatrix}, \qquad c > 0$

Let us propose the following Lyapunov function

$$H = \frac{1}{2}\tilde{X}^T D\tilde{X} + \frac{1}{2\gamma}\tilde{\theta}^2$$

Where $\gamma > 0$

Its time derivative along the trajectories of (25) gives

$$\dot{H} = \tilde{X}^T D \dot{\tilde{X}} + \frac{1}{\gamma}\tilde{\theta}\dot{\tilde{\theta}}$$

$$= -\tilde{X}^T (R+C)\tilde{X} + \left[(v_0 - v_{0d})v_{0d} + \frac{1}{\gamma}\dot{\tilde{\theta}} \right]\tilde{\theta}$$

Define the adaptive law

$$(v_0 - v_{0d})v_{0d} + \frac{1}{\gamma}\dot{\tilde{\theta}} = 0$$

Therefore

$$\hat{\theta} = \int \gamma \cdot v_{0d}(v_{0d} - v_0)dt \qquad (27)$$

Under this condition

$$\dot{H} = -\tilde{X}^T (R+C)\tilde{X} < 0$$

Hence $\lim_{t\to\infty} \tilde{X} = 0, \qquad v_0 \to v_{0d}$

Similarly the control law is obtained from (26)

$$I = \hat{\theta}v^* + c(v^* - v_0) - cLC_1 \frac{d^2 v_0}{dt^2} \qquad (28)$$

Where $v^* = v_{0d}$ is the desired value of the output voltage. Therefore (28) and (27) construct the passivity-based adaptive controller. It performs the global asymptotic regulation of the output voltage perturbed by different values of resistance load. The convergence rate is related to the coefficient c.

V Simulation and Experiment

A DC voltage applied to the resonant converter as shown in Fig. 1 is derived by a full bridge rectifier with large capacitor filter, the input DC voltage is E=311 V. The desired output voltage is 140 V. The power rating of the converter is 1.4 kW which corresponds to the load resistance r=14 Ω. The inductance and capacitance in the resonant circuit are Lr=56 μH, Cr=0.5 μF, respectively. This corresponds to a resonant frequency fr=30.1 kHz. The switching frequency is fs=33 kHz，Under this circumstance the resonant current is quite sinusoidal and it is lagging the output voltage of the full bridge, this treatment is helpful for the soft switching of the converter to increase efficiency. Fig. 4 shows the waveform of the resonant current. It confirms the first harmonic approximation of the system is reasonable. The output filter has the following parameters: C1=C2=100μF, L=200μH. The PBC controller is implemented, as well as the classic PI controller in order to compare their dynamic performance and robustness under similar conditions. The design parameters of the two controllers were obtained from experiments where we choose the set of parameters which exhibits the better response in time domain. For the PI controller, the set of parameters are Kp=0.0002, Ki=0.03. For the adaptive version PBC controller, the damping coefficient and the adaptive gain are tuned to be c=0.2, γ=0.003, respectively. The sampling time is 100 μs. Based on above parameters, simulations and experiments were performed respectively.

A Simulation

The simulations were carried out on Simulink/Matlab. In order to test the dynamic performance and robustness of the control system we simulated the whole process including starting with half load (load resistance r=28 Ω), step change in the load resistance from r=28 Ω to r=14 Ω and step change in the load resistance from r=14 Ω to r=28 Ω. The desired output voltage is 140 V.

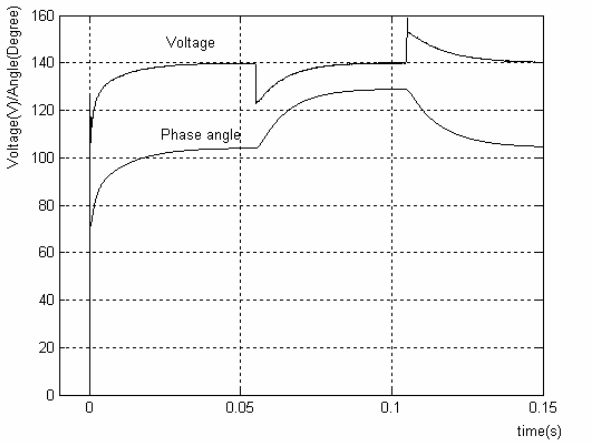

Fig. 5 Simulation waveforms

The upper curve in Fig. 5 is the response of the output voltage and the other one is of the corresponding phase angle α, the curves show the performance of the system to against load disturbance, the simulation results are agree with the experimental results which will be described bellow.

B Experiment results

A DSP-based interface where the controller is programmed is employed and plugged into a PC in order to access the information and download the control program. The experiments were aim at exhibiting the behavior of the controller with respect to step changes in desired output voltage and also with respect to step changes in load disturbance, which is considered unknown for the controller.

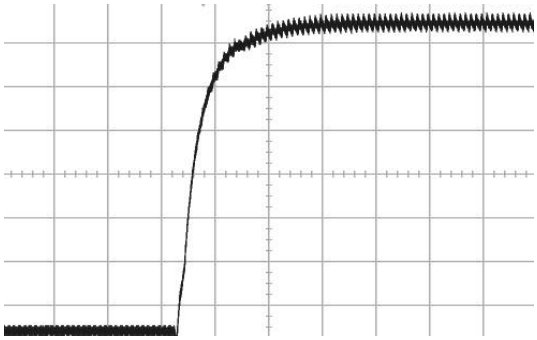

Fig. 6 PI controller, response of output voltage
When starting, 20V/div, 100ms/div

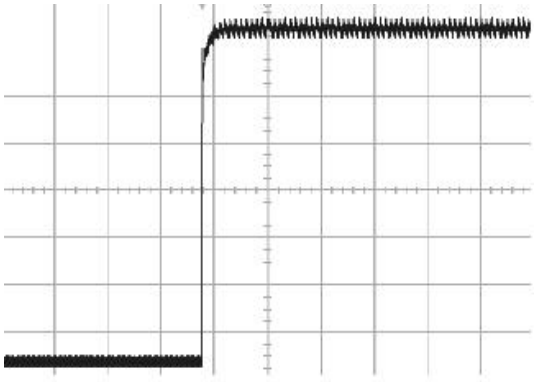

Fig. 7 PBC controller, response of output voltage
When starting, 20V/div, 100ms/div

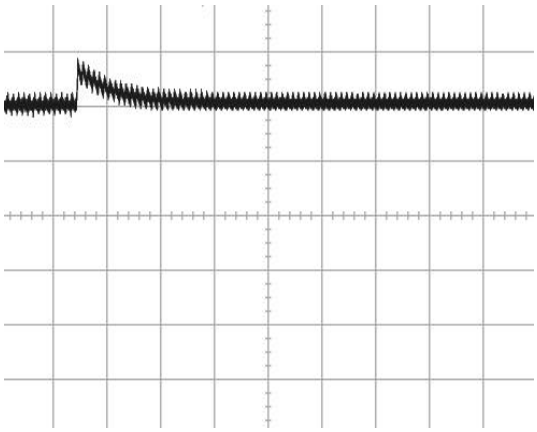

Fig. 8 PI controller, response of output voltage
to a step change in r from 14 Ω to 28 Ω
20V/div, 100ms/div

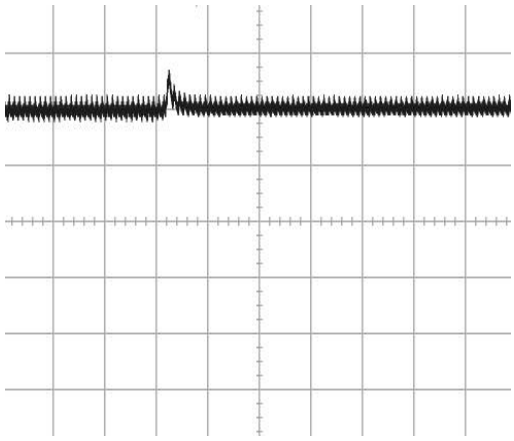

Fig. 9 PBC controller, response of output voltage
to a step change in r from 14 Ω to 28 Ω
20V/div, 100ms/div

Two sets of experiment will be used for this study. In the first set of experiments, we try to compare the response of the output voltage when step changes in desired output voltage occur respect to different controllers, the desired output voltage is step changed from 0 Volt to the rated voltage 140 Volts, the load resistance is maintained at r=28 Ω, the response shown in Fig. 6 is faster than that in Fig. 7. The dynamic performance of starting of the converter employing PBC controller is better than that employing classic PI controller, both of them are with none steady errors in the output voltage response.

The second set of experiments is that the load is changed from 1.4 kW to 0.7 kW which corresponds to a step change in the load resistance from r=14 Ω to r=28 Ω, respectively. Fig. 8 and Fig. 9 are the curves of output voltage while load disturbance happened for the PI controller and PBC controller, respectively. It can be seen from the two figures that the settling time are around 100ms and 30ms, respectively, and the overshoots are about 18V and 14V, respectively.

Generally the settling time and overshoot or voltage drop are ambivalent in the system with classic controller, the cost of improving one is always scarifying the other one. Notice that the response of the output voltage of the converter employing PBC controller achieves faster

rejection of this type of disturbance when their overshoots are almost identical. Nevertheless, we observe from above experimental results that that the PBC controller exhibits its better ability to regulate the voltage variation caused by the load perturbations. It is important for some loads such as electronic apparatus.

Ⅵ Conclusion

The H-bridge resonant converter has been examined for the PBC and PI control method. A set of equation has been formulated and developed for the PBC control. The salient point of the method is that only single loop is used for control. A load observer is derived to ensure the controller is effective in the event of large load disturbance. Experimental results are presented to illustrate the features of the passivity-based control and PI control in the converter.

References

[1] D. M. Sable, and F. C. Lee, The operation of a full bridge, zero-voltage-switched PWM converter, Proceedings of Virginia Power Electronics Center Seminar, 1989, pp. 92-97.

[2] A. J. Forsyth, P. D. Evans, M. R. D. Al-Mothafar and K. W. E. Cheng, "A Comparison of phase-shift controlled resonant and square-wave converters for high power ion engine control", European Space Power Conference, 1991, pp. 179-185.

[3] Chan H.L., Cheng K.W.E., and Sutanto D., "Phase-shift controlled DC-DC converter with bi-directional power flow**",** IEE Proceedings-Electr. Power Appl., Vol. 148, No. 2, March 2001, pp. 193-201.

[4] A.J.Forsyth, P.D.Evans, K.W.E.Cheng and M.R.D.Al-Mothafar, 'Operating limits of power converters for high power ion engine control', 22nd Int. Electric Propulsion Conference, 1991.

[5] A. M. Stankovic, D. J. Perreault, and K. Sato, "Analysis and experimentation with dissipative nonlinear controllers for serious resonant dc/dc converters," in Proc. 28th Annu. IEEE Power Electron. Spec.Conf. (PESC97), vol. 1, St. Louis, MI, May 1997, pp. 679-685.

[6] Carrasco, J.M.; Galvan, E.; Valderrama, G.E.; Ortega, R.; Stankovic, A.M,;"Analysis and experimentation of nonlinear adaptive controllers for the series resonant converter," IEEE Trans. Power Electronics, vol. 15, pp. 536 – 544, May. 2000.

[7] H. Sira-Ramirez, R. Ortega, R.A. Perezmoreo and M. Garcia-Esteban, "Passivity-Based Controllers for the Stabilization of DC-to-DC Power Converters," Automatica, 1995, submitted.

[8] R. Ortega, A. Loria, P. J. Nicklasson, and H. Sira-Ramirez, Passivity-Based Control of Euler-Lagrange Systems. Berlin, Germany: Springer-Verlag, 1998.

[9] R.Ortega, G.Espinosa, "Torque Regulation of Induction Motors," Automatica, Vol.29, No.3, pp621-633, 1993.

[10] H. Sira-Ramirez, R. Ortega, and M. Garcia-Esteban, "Adaptive passivity-based control of average dc-to-dc power converter models," Int.J. Adaptive Contr. Signal Processing, vol. 12, pp. 63-80, 1998.

[11] Escobar, G.; Chevreau, D.; Ortega, R.; Mendes, E.;" An adaptive passivity-based controller for a unity power factor rectifier," IEEE Trans. Control Systems Technology, vol. 9, issue: 4, pp. 637-644, July, 2001

Acknowledgement

The authors gratefully acknowledge the support of the RGC, Hong Kong for the paper (PolyU5103/01E and Research Office of the Hong Kong Polytechnic University (Project no B-Q474).